TECHNICAL REPORT BRL-TR-3084

BRL

ACCURACY OF VULNERABILITY INTEGRALS

AIVARS CELMIŅŠ

APRIL 1990

U.S. ARMY LABORATORY COMMAND

BALLISTIC RESEARCH LABORATORY
ABERDEEN PROVING GROUND, MARYLAND

NOTICES

Destroy this report when it is no longer needed. DO NOT return it to the originator.

Additional copies of this report may be obtained from the National Technical Information Service, U.S. Department of Commerce, 5285 Port Royal Road, Springfield, VA 22161.

The findings of this report are not to be construed as an official Department of the Army position, unless so designated by other authorized documents.

The use of trade names or manufacturers' names in this report does not constitute indorsement of any commercial product.

REPORT DOCUMENTATION PAGE

Form Approved
OMB No. 0704-0188

1. AGENCY USE ONLY (Leave blank)	2. REPORT DATE	3. REPORT TYPE AND DATES COVERED
	April 1990	Final, 3 Apr 89 - 32 Oct 89

4. TITLE AND SUBTITLE
Accuracy of Vulnerability Integrals

5. FUNDING NUMBERS
44592-001-07-2501

6. AUTHOR(S)
Aivars Celmiņš

7. PERFORMING ORGANIZATION NAME(S) AND ADDRESS(ES)

8. PERFORMING ORGANIZATION REPORT NUMBER

9. SPONSORING / MONITORING AGENCY NAME(S) AND ADDRESS(ES)
US Army Ballistic Research Laboratory
ATTN: SLCBR-DD-T
Aberdeen Proving Ground, MD 21005-5066

10. SPONSORING / MONITORING AGENCY REPORT NUMBER
BRL-TR-3084

11. SUPPLEMENTARY NOTES

12a. DISTRIBUTION / AVAILABILITY STATEMENT
Approved for public release; distribution unlimited.

12b. DISTRIBUTION CODE

13. ABSTRACT *(Maximum 200 words)*

This report investigates the accuracy of vulnerability indicators that represent average vulnerability either over a threat dispersion area or over the silhouette of a target. Mathematically, these indicators are surface integrals of local vulnerability over a reference plane normal to the direction of the threat. In applications, the integrals are computed by discrete numerical integration. The accuracy of the resulting indicators depends on the accuracy of the local vulnerability, the detail of the target description and on the properties of the numerical integration method. This report provides error estimates for the latter two error sources. The estimates help one to determine the appropriate target detail and integration procedure so that the overall accuracy of the vulnerability indicator is at the achievable level.

14. SUBJECT TERMS
Vulnerability accuracy
Monte Carlo computation
Integration cell size
Detail of target description
Average vulnerability
Vulnerable area

15. NUMBER OF PAGES
42

16. PRICE CODE

17. SECURITY CLASSIFICATION OF REPORT	18. SECURITY CLASSIFICATION OF THIS PAGE	19. SECURITY CLASSIFICATION OF ABSTRACT	20. LIMITATION OF ABSTRACT
UNCLASSIFIED	UNCLASSIFIED	UNCLASSIFIED	SAR

NSN 7540-01-280-5500

Standard Form 298 (Rev 2-89)
Prescribed by ANSI Std Z39-18
298-102

GENERAL INSTRUCTIONS FOR COMPLETING SF 298

The Report Documentation Page (RDP) is used in announcing and cataloging reports. It is important that this information be consistent with the rest of the report, particularly the cover and title page. Instructions for filling in each block of the form follow. It is important to *stay within the lines* to meet *optical scanning requirements*.

Block 1. Agency Use Only *(Leave blank)*.

Block 2. Report Date. Full publication date including day, month, and year, if available (e.g. 1 Jan 88). Must cite at least the year.

Block 3. Type of Report and Dates Covered. State whether report is interim, final, etc. If applicable, enter inclusive report dates (e.g. 10 Jun 87 - 30 Jun 88).

Block 4. Title and Subtitle. A title is taken from the part of the report that provides the most meaningful and complete information. When a report is prepared in more than one volume, repeat the primary title, add volume number, and include subtitle for the specific volume. On classified documents enter the title classification in parentheses.

Block 5. Funding Numbers. To include contract and grant numbers; may include program element number(s), project number(s), task number(s), and work unit number(s). Use the following labels:

C	- Contract	PR	- Project
G	- Grant	TA	- Task
PE	- Program Element	WU	- Work Unit Accession No.

Block 6. Author(s). Name(s) of person(s) responsible for writing the report, performing the research, or credited with the content of the report. If editor or compiler, this should follow the name(s).

Block 7. Performing Organization Name(s) and Address(es). Self-explanatory.

Block 8. Performing Organization Report Number. Enter the unique alphanumeric report number(s) assigned by the organization performing the report.

Block 9. Sponsoring/Monitoring Agency Name(s) and Address(es). Self-explanatory.

Block 10. Sponsoring/Monitoring Agency Report Number. *(If known)*

Block 11. Supplementary Notes. Enter information not included elsewhere such as: Prepared in cooperation with. ; Trans. of ..; To be published in . When a report is revised, include a statement whether the new report supersedes or supplements the older report.

Block 12a. Distribution/Availability Statement. Denotes public availability or limitations. Cite any availability to the public. Enter additional limitations or special markings in all capitals (e.g. NOFORN, REL, ITAR).

- DOD - See DoDD 5230.24, "Distribution Statements on Technical Documents."
- DOE - See authorities.
- NASA - See Handbook NHB 2200.2.
- NTIS - Leave blank.

Block 12b. Distribution Code.

- DOD - Leave blank.
- DOE - Enter DOE distribution categories from the Standard Distribution for Unclassified Scientific and Technical Reports.
- NASA - Leave blank.
- NTIS - Leave blank.

Block 13. Abstract. Include a brief *(Maximum 200 words)* factual summary of the most significant information contained in the report.

Block 14. Subject Terms. Keywords or phrases identifying major subjects in the report.

Block 15. Number of Pages. Enter the total number of pages.

Block 16. Price Code. Enter appropriate price code *(NTIS only)*.

Blocks 17. - 19. Security Classifications. Self-explanatory. Enter U.S. Security Classification in accordance with U.S. Security Regulations (i.e., UNCLASSIFIED). If form contains classified information, stamp classification on the top and bottom of the page.

Block 20. Limitation of Abstract. This block must be completed to assign a limitation to the abstract. Enter either UL (unlimited) or SAR (same as report). An entry in this block is necessary if the abstract is to be limited. If blank, the abstract is assumed to be unlimited.

TABLE OF CONTENTS.

INTENTIONALLY LEFT BLANK.

1. Introduction

Given the type of a threat and its attack direction the vulnerability of a target system (e.g. of a tank) is computed in two steps. First, one computes estimates of the effect of the threat for a number of attack points. Second, these effects are integrated to obtain the overall effect. The evaluation of the integrals is done by a summation of the local effects and the result of the integration measures the overall "vulnerability" of the target. Depending on the definitions of the local effects and the form of the integrals the computed result might be a "vulnerable area", a "probability of kill" or another similar averaged vulnerability indicator. The accuracy of the result depends on the following three parts of the computing process: the accuracy of the local vulnerability model, the detail and accuracy of the target description and the accuracy of the numerical evaluation of the integrals. In a reasonable procedure, these three sources of inaccuracies should be properly balanced. The present report provides criterions and error estimates that help one to achieve such a balance. For instance, using the results of this report one can determine if improvement of any part of the calculations is indicated, or whether a contemplated improvement will have a noticeable effect on the overall accuracy of the computation.

Usually the numerical evaluation of the integrals is done by defining a computing grid with square cells in a reference plane normal to the direction of the threat, computing the integrands at a random point in each cell and approximating the surface integrals by appropriately weighted sums over the computing cells. The discretization error will decrease for smaller cell sizes and, therefore the cell sizes should be small. On the other hand, the detail of the target is finite, and sometimes the target description is quite coarse. This means, that for a given target there is a bound for the cell sizes in the sense that any calculations with smaller cells do not change the value of the integral, because in a very fine net the integrand is constant within most of the cells. Consequently, there is also a bound for the accuracy of the vulnerability indicators which cannot be improved by refined numerical integration. That bound depends on the detail of the target description, on the spacial variation of the response of the various components of the target to the threat, and on the accuracy of the local vulnerability models. Our task is to find this bound in terms of easily obtainable input information. The largest cell size that produces the integral value with the achievable accuracy can be considered as an optimal cell size. Also useful are accuracy estimates for computations with cell sizes that are larger than the optimum. Then the accuracy can be improved by sampling at more than one point from each cell, and one would like to have an estimate of the proper number of samples.

We illustrate some aspects of the problem using a one-dimensional example where the problem is easily tractable. Let $y=h(x)$ be a piecewise constant function, and let f_j be the

sum of lengths of segments where $y=h_j=constant$. Then (see Figure 1)

$$I = \int_a^b h(x)\,dx = \sum_{j=1}^{c} f_j\, h_j \quad . \tag{1.1}$$

Let the values h_j have uncertainties which are expressed by spreads δh_j. The corresponding spread of the integral is

$$\delta I = \sum_{j=1}^{c} f_j\, \delta h_j \quad . \tag{1.2}$$

We compute the integral numerically by subdividing the segment $b-a$ into n equal elementary segments and sampling the integrand at k random points in each elementary segment. The average distance between the sampling points is

$$\delta = \frac{b-a}{n\,k} \quad , \tag{1.3}$$

and the integral is approximated by

$$\bar{I} = \frac{b-a}{n\,k} \sum_{i=1}^{n} \sum_{l=1}^{k} h(x_{il}) \quad , \tag{1.4}$$

where x_{il} are the coordinates of the sampling points in the i-th segment. We bound the difference between $\bar{I}$ and I by considering points of discontinuity of $h(x)$. Let $\{b\}$ be the set of all those elementary segments which contain at least one discontinuity, and let Δh_j be the range of $h(x)$ within the elementary segment j. Then

$$|\,\bar{I} - I\,| \le D = \frac{b-a}{n} \sum_{j\in\{b\}} \Delta h_j \quad . \tag{1.5}$$

The sample size parameter k does not enter the expression (1.5) for the bound of the difference, because the x_{il} are chosen at random in each elementary segment.

Next we derive three estimates for the standard deviation $\sigma(\bar{I})$ of the approximation $\bar{I}$ from the true value I. Each estimate is based on different assumptions about the integrand and the arrangement of the sampling points. We show in the Appendix that for a random arrangement of nk sampling points the standard deviation is bounded by

$$\sigma(\bar{I}) \le \frac{b-a}{\sqrt{nk}} \left[\, (h_{max}-\bar{h})(\bar{h}-h_{min}) \,\right]^{1/2} \le \frac{b-a}{\sqrt{nk}}\, \frac{1}{2}\, (h_{max}-h_{min}) \quad , \tag{1.6}$$

where $\bar{h}$ is the average value of $h(x)$. This estimate only requires that the integral I exists and no other properties of $h(x)$ are used.

A better estimate is obtained if one takes into account the piecewise-constant property of the integrand. Then the sum (1.4) can be rearranged as follows

$$\bar{I} = (b-a) \sum_{j=1}^{c} a_j h_j \quad , \tag{1.7}$$

where a_j is the fraction of sampling points that fall within the segment f_j. The expected value of a_j is $f_j/(b-a)$ and the standard deviation of a_j is (Ref. 1, p. 168)

$$\sigma(a_j) = \frac{1}{\sqrt{nk}} \left[a_j \, (1-a_j) \right]^{1/2} \quad . \tag{1.8}$$

Hence

$$\sigma(\bar{I}) = (b-a) \left[\sum_{j=1}^{c} \sigma(a_j)^2 \, (h_j - \bar{h})^2 \right]^{1/2} = \frac{1}{\sqrt{nk}} \left[\sum_{j=1}^{c} f_j(1-f_j)(h_j-\bar{h})^2 \right]^{1/2} . \tag{1.9}$$

For the third formula we assume that the integrand is piecewise constant and that the n elementary segments are equal. In each elementary segment the k sampling points are random and we may use eq. (1.6) to estimate the standard deviation of integration over the segment. Let I_i be the integral of $h(x)$ over the i-th elementary segment, $\bar{h}_i$ be the average value of $h(x)$ within the segment, and $\bar{I}_i = (b-a)\bar{h}_i/n$. Then, in analogy to eq. (1.6)

$$\sigma(\bar{I}_i) \le \frac{b-a}{n} \frac{1}{\sqrt{k}} [\, (h_{i\max} - \bar{h}_i)(\bar{h}_i - h_{i\min}) \,]^{1/2} \le \frac{b-a}{n\sqrt{k}} \, \frac{1}{2} \, \Delta h_i \quad . \tag{1.10}$$

Hence an estimate of the standard deviation of $\bar{I}$ is

$$\sigma(\bar{I}) = \left(\sum_{i \in \{b\}} \sigma^2(\bar{I}_i) \right)^{1/2} \le \frac{b-a}{n\sqrt{k}} \, \frac{1}{2} \left(\sum_{i \in \{b\}} (\Delta h_i)^2 \right)^{1/2} \quad . \tag{1.11}$$

If n is sufficiently large then the estimate (1.11) is better (smaller) than the estimate (1.9). This is so because in the derivation of eq. (1.11) we have used more information about the computing process.

The number of sampling points should be sufficiently large so that the error of the numerical integration is smaller than the intrinsic error of the integral. Therefore, one should chose n such that

$$D < \delta I \quad , \tag{1.12}$$

or chose n and k such that, using one of the estimates for σ,

$$\sigma(\bar{I}) < \delta I \quad , \tag{1.13}$$

or less than a fraction of δI. The second condition (1.13) is less demanding, because it uses an estimate of the standard deviation of the integral, whereas the condition (1.12) is based on a bound of the integration error.

A function step with $y = h_j$ and the width t_j contributes $(h_j - h_0)t_j$ to the value of the integral, whereby h_0 is the average value of y within the segment t_j if the step is left out. It is not reasonable to include the step into the definition of the function if

$$| (h_j - h_0)\, t_j | \ll \delta I \tag{1.14}$$

or if

$$| (h_j - h_0)\, t_j | \ll \sigma(\bar{I}) \ . \tag{1.15}$$

In the example shown in Figure 1 the step of the integrand with the width f_5 contributes to the integral less than δI (half of the shaded area). Therefore, this step can be deleted without a noticeable effect on the integral value. This criterion for a deletion or inclusion of a step into the integrand depends only on the accuracy of the integrand and is independent of the integration method. An example of a border case is the step with the width f_2. Its contribution to the integral is approximately equal to the spread δI and, therefore, it should be kept in the integrand.

To capture all relevant parts of the integrand, the distance between sampling points should be less than the width f of the smallest relevant step of $h(x)$. In terms of the average distance (1.3) the condition is

$$\frac{b-a}{nk} < \frac{1}{2} f \ . \tag{1.16}$$

More rigorous is the condition in terms of the maximum distance between sampling points:

$$\frac{b-a}{n} < \frac{1}{2} f \ . \tag{1.17}$$

The conditions (1.16) or (1.17) for the number of sampling points are based on the detail of the function $h(x)$, whereas the conditions (1.12) and (1.13) are based on the accuracy of the function. Hence, each set of conditions address different aspects of the problem and supplement each other.

In the remaining part of this report we apply the outlined considerations to the surface integrals of vulnerability computations. To simplify the analysis we assume that the number of computing cells or sampling points is large (at least of the order of 100) since this is usual in applications. The integral formulation of vulnerability indicators is provided in Section 2, where we also discuss the inaccuracies of the vulnerability integrals in terms of the inaccuracies of the predicted local effects. From that discussion, we establish criterions for the inclusion of (small) additional components into a given target description. Formulas for the numerical evaluation of the integrals by sampling are given in Section 3. The section also contains accuracy estimates for the integrals based on the number of sampling points. In Section 4 we discuss the accuracy of the numerical evaluation of the integrals in terms of the properties of the integrand. Conditions are derived for the size of the integration cells and for the number of samples which insure that the target geometry is properly taken into account. The accuracy estimates of Section 3 are specialized in Section 5, where we take into account the piecewise-constant property of the integrand. A further refinement is provided in Section 6, where also the cellular arrangement of the sampling points is exploited. In Section 7 we illustrate the application of the results by presenting an example where the proper cell sizes and/or number of sampling points are

estimated. A summary of the results and conclusions are given in Section 8.

2. Integral Formulation of Vulnerability Indicators

We consider the vulnerability of a target system, such as a tank with respect to a threat from a particular direction. To the threat, the target presents an area (a silhouette) within which the threat might have an effect. The silhouette is the projection of the outline of the target onto a plane normal to the direction of the threat. We call this plane the *reference plane*. In the vicinity of the target the threat is assumed to travel along a straight path called a shotline. Each shotline is normal to the reference plane and completely described by the coordinates x and y of its intersection with the plane. If a shotline of an attacking threat falls within the silhouette of the target then the threat might have a non-zero effect which we assume can be calculated and which we denote by $v(x,y)$. We further assume that the effect function $v(x,y)$ is dimensionless and has a value between zero and one. The overall vulnerability of the target to a threat from a direction normal to the reference plane is obtained by integrating the effect $v(x,y)$ over the reference plane. The effect may be, for instance the probability of kill or the reduction of combat effectiveness, and the integral over $v(x,y)$ can be either simple or weighted (the latter if an average of v is computed). The threat might also have a distribution in the reference plane, specified for instance by an aim point and a dispersion. Then the vulnerability integral is a weighted average of $v(x,y)$ with the distribution density of the threat as weight.

We define two generic vulnerability integrals which represent two types of vulnerability indicators. Let E be the reference plane, S be the area of the silhouette in E and let $v(x,y)$ be the probability of kill. We call the first integral the *vulnerable area* and define it by

$$V_S = \int_S v(x,y)\, dx\, dy \quad . \tag{2.1}$$

The dimension of V_S is m^2.

The second vulnerability integral represents an average of the effect function $v(x,y)$ over an averaging area. That area usually is either the silhouette of the target or a dispersion area of the threat. We assume that the averaging area and the averaging weight are specified by a weight density function $g(x,y)$ that has the dimension $1/m^2$ and is normalized by

$$\int_E g(x,y)\, dx\, dy = 1 \, . \tag{2.2}$$

We define the *average vulnerability* V_A by

$$V_A = \int_A g(x,y)\, v(x,y)\, dx\, dy \quad , \tag{2.3}$$

where A is the area defined by $g(x,y)>0$. We introduce a dimensionless weight function $\gamma(x,y)$ by the definition

$$\gamma(x,y) = g(x,y) \cdot A \quad . \tag{2.4}$$

Then the average vulnerability is

$$V_A = \frac{1}{A} \int_A \gamma(x,y)\, v(x,y)\, dx\, dy \quad . \tag{2.5}$$

We assume that the function $g(x,y)$ is exactly known, differentiable in A and has a bounded gradient in A. About $v(x,y)$ we assume that it might contain unknown errors with absolute values less than a given error bound function $\delta v(x,y)$. For simplicity, we assume a symmetric error bound with the property

$$\delta v(x,y) \le \min \{ v(x,y), 1-v(x,y) \} \quad , \tag{2.6}$$

so that

$$0 \le v(x,y)-\delta v(x,y) \le v(x,y)+\delta v(x,y) \le 1 \quad . \tag{2.7}$$

The intrinsic error of V_S due to the inaccuracies of $v(x,y)$ is bounded by

$$\delta V_S = \int_S \delta v(x,y)\, dx\, dy \quad . \tag{2.8}$$

Next, we subdivide the silhouette S in sub-areas F_j such that within each F_j the effect function is approximately constant. Often these areas will coincide with presented areas of target components, particularly in so-called compartment model calculations. In general they will be extensions, combinations or parts of component projections. Let the F_j be called *nodal areas* and the corresponding constant values $\bar{v}_{Fj}$ of the effect function be called *nodal values* of $v(x,y)$. Formally, we define the F_j as follows. F_j, $j=1,\ldots,c$ is a set of areas such that $F_j \cap F_i = 0$ if $j \neq i$, $\bigcup_j F_j \subseteq S$ and $|\, v(x,y)-\bar{v}_{Fj} | \le \Delta v_{Fj}/2$ for (x,y) in F_j, whereby $\bar{v}_{Fj}>0$ is the average value of $v(x,y)$ in F_j, and the Δv_{Fj} are arbitrary but fixed constants. We supplement this set with a nodal area F_0 which encloses all those parts of the silhouette and reference plane where $\bar{v}_{F0}=0$. In terms of the nodal areas the vulnerable area is

$$V_S = \sum_{j=1}^{c} \int_{F_j} v(x,y)\, dx\, dy = \sum_{j=1}^{c} F_j\, \bar{v}_{Fj} \quad . \tag{2.9}$$

The error bound (2.8) can be further bounded using the F_j by

$$\delta V_S \le D_S = \sum_{j=1}^{c} F_j\, \delta v_{Fj\max} \quad , \tag{2.10}$$

where $\delta v_{Fj\max}$ is the maximum value of $\delta v(x,y)$ in the nodal area F_j.

The nodal value representation (2.9) of the vulnerability integral is not merely an artifact. Such a representation is natural for compartment model calculations where $v(x,y)$ is approximately constant within the projections of component silhouettes onto E. Also, recent high resolution calculations that include spall modeling indicate that $v(x,y)$ likely in general assumes only a finite number of values. Examples and an explanation of this property of $v(x,y)$ are given in Reference 2, page 35.

Eqs. (2.8) or (2.10) can be used to determine whether a particular component should be added to an existing target description. Let the *effective presented area* of a component be that part of E in which the threat has an effect on the component. In a compartment model, the effective presented area is the projection of the silhouette of the component onto E. In a general model, particularly if spall effects are considered, the effective presented area will be larger than the silhouette. Let T_j be the effective presented area of a component, $\bar{v}_{Tj}$ be the average value of $v(x,y)$ within T_j, $\bar{v}_{0j}$ be the average within T_j before the component is added, and δv_{Tjmax} be the maximum of δv within T_j. Then a reasonable criterion for the inclusion of the component into the target description is

$$\left.\begin{aligned} |T_j \cdot (\bar{v}_{Tj} - \bar{v}_{0j})| \;&> \frac{1}{2} D_s \\ \text{or} \qquad T_j \cdot \delta v_{Tjmax} \;&> \frac{1}{2} D_s \;. \end{aligned}\right\} \tag{2.11}$$

The second condition in (2.11) is included to cover cases where the addition of the new component does not significantly change the value of V_s, but nevertheless increases the inaccuracy of the result. The exclusion of such a component would falsely suggest a too accurate result.

Corresponding formulas for the average vulnerability V_A are as follows.

$$\delta V_A = \frac{1}{A} \int_A \gamma(x,y)\, \delta v(x,y)\, dx\, dy \;, \tag{2.12}$$

$$V_A = \frac{1}{A} \sum_{j=0}^{e} (F_j \cap A) \cdot \overline{(\gamma v)}_{Fj} \;, \tag{2.13}$$

$$\delta V_A \le D_A = \frac{1}{A} \sum_{j=0}^{e} (F_j \cap A) \cdot [\gamma\, \delta v]_{Fjmax} \;. \tag{2.14}$$

The summation in eqs. (2.13) and (2.14) starts with $j=0$ because the nodal area with $\bar{v}_{Fj}=0$ must be included in the sum. The total number of nodal areas intersecting with A, $e+1$, in general will be less than the number c of nodal areas intersecting with the silhouette. The criterion for the inclusion of a component with the effective presented area T_j in the target description is

$$\left.\begin{aligned} &\left| T_j \cdot \frac{1}{A} \cdot \{ \overline{(\gamma v)}_{Tj} - \overline{(\gamma v)}_{0j} \} \right| > \frac{1}{2} D_A \\ \text{and} \quad &T_j \cdot \frac{1}{A} \cdot [\gamma \, \delta v \,]_{Tj\max} > \frac{1}{2} D_A \ . \end{aligned}\right\} \tag{2.15}$$

Parts of nodal areas which satisfy the conditions (2.11) or (2.15), respectively, we call *relevant*. One can use these criterions to simplify target descriptions so that all parts of nodal areas are relevant. In particular, the criterions can help to simplify complicated boundaries of nodal areas. We note that in certain problems there can be other criterions which justify the inclusion of small nodal areas in a target description. For instance, if the target contains a large number of irrelevant components which cannot be easily combined into a few components with simple geometry, and whose combined contribution is relevant, then one might treat all components as relevant. However, as we shall see later, if the relevent details are very small, then one needs a very long computing time to capture their small contributions. Therefore, it is advisable to keep the target description simple, smoothing out complicated component boundaries and combining small components into larger and simpler ones. Because only approximate estimates of D_S, D_A and of the other terms in the criterions (2.11) and (2.15) are needed, the estimates can be obtained by visual inspection of temporary results with few and simple components.

3. Monte Carlo Computation of Vulnerability Integrals

The computation of a value of the effect function $v(x,y)$ typically involves tracing the shotline with the coordinates (x,y) through the target and evaluating the damage models for those target components which are encountered by the shotline or otherwise affected, e.g. by spall. The results from the damage models are aggregated by special algorithms to obtain the effect $v(x,y)$ of the threat on the target system. Because $v(x,y)$ can only be obtained pointwise, the vulnerability integrals are computed by discrete approximations. Usually this is done by defining in the reference plane a square grid, obtaining a value of $v(x,y)$ for a randomly chosen point within each cell of the grid, and adding the values with appropriate weights according to eq. (2.1) or (2.5), respectively.

For a general grid consisting of identical cells, the algorithm can be described as follows. Let C [m^2] be the area of a cell in the computing grid and n be the number of cells within the silhouette. Let (x_i,y_i) be a point in the i-th computing cell. Then the approximation of the vulnerable area integral is

$$\bar{V}_S = C \sum_{i=1}^{n} v(x_i,y_i) = \frac{S}{n} \sum_{i=1}^{n} v(x_i,y_i) \ , \tag{3.1}$$

where the summation is over the n cells that intersect with the target silhouette. The approximation of the average vulnerability integral is

$$\bar{V}_A = \frac{C}{A} \sum_{i=1}^{m} \gamma(x_i,y_i)\, v(x_i,y_i) = \frac{1}{m} \sum_{i=1}^{m} \gamma(x_i,y_i)\, v(x_i,y_i) \quad , \tag{3.2}$$

where m is the number of cells that intersect with A.

A simple generalization of the algorithms is to take more than one sample of the integrand from each computing cell. Let k be the number of samples from each cell, let (x_{il},y_{il}) be points within the i-th cell and let $v_{il}=v(x_{il},y_{il})$. Then the approximate vulnerable area integral is

$$\bar{V}_S = C\, \frac{1}{k} \sum_{i=1}^{n} \sum_{l=1}^{k} v_{il} = S\, \frac{1}{nk} \sum_{i=1}^{n} \sum_{l=1}^{k} v_{il} \quad , \tag{3.3}$$

and the approximate average vulnerability integral is

$$\bar{V}_A = \frac{C}{A}\, \frac{1}{k} \sum_{i=1}^{m} \sum_{l=1}^{k} \gamma_{il}\, v_{il} = \frac{1}{mk} \sum_{i=1}^{m} \sum_{l=1}^{k} \gamma_{il}\, v_{il} \quad . \tag{3.4}$$

Equations (3.3) and (3.4) include as special cases eqs. (3.1) and (3.2).

Estimates of the standard deviation of a numerically computed integral from its true value are derived in the Appendix. The estimated standard deviation of the approximation $\bar{V}_S$ to the vulnerable area integral V_S is

$$\sigma(\bar{V}_S) \le \frac{S}{\sqrt{nk}} \left[\left(1 - \frac{\bar{V}_S}{S}\right) \frac{\bar{V}_S}{S} \right]^{1/2} \le \frac{S}{\sqrt{nk}}\, \frac{1}{2} = \frac{s\sqrt{S}}{2\sqrt{k}} \quad , \tag{3.5}$$

where $s=\sqrt{C}=(S/n)^{1/2}$ is the side length of a computing cell if the grid consists of square cells. An estimate of the standard deviation of the approximation $\bar{V}_A$ to the average vulnerability V_A is

$$\sigma(\bar{V}_A) \le \frac{1}{\sqrt{mk}} \left[\left(\Gamma - \bar{V}_A\right) \bar{V}_A \right]^{1/2} \le \frac{1}{\sqrt{mk}}\, \frac{1}{2} = \frac{s}{2\sqrt{k}\,\sqrt{A}} \quad , \tag{3.6}$$

where Γ is the largest value of $\gamma(x,y)$ within the intersection of A and S.

The standard deviation estimates (3.5) and (3.6) are general assuming only that the range of $v(x,y)$ is the interval [0,1] and that the sampling points are random. One can obtain other estimates by also taking into account the piecewise-constant nature of the integrand and the cellular arrangement of the sampling points. We shall derive such estimates in later sections of this report. However, their usefulness is likely restricted to simple target geometries, because the application of the formulas require an analysis of the target description.

4. Cell Size Commensurate with Target Description

In Section 2 we introduced a subdivision of the target silhouette in nodal areas F_j with approximately constant $v(x,y)$ in each area. The proper cell size for the numerical evaluation of vulnerability integrals depends on the size and shape of these areas. On one hand, the cells should be sufficiently small to capture complicated boundaries of the nodal areas. On the other hand, small slender extensions from a nodal area do not contribute significantly to the values of the integrals. We characterize the smoothness of the boundaries of nodal areas by a parameter that expresses the fineness of the details of the boundaries. We loosely define the parameter as the average diameter of the smallest relevant convex part of the nodal area F_j and call it the *fineness* f_j of the nodal area F_j. (The relevance of parts of nodal areas are discussed at the end of Section 2). The *fineness of the target description* is defined as the smallest f_j :

$$f = \min_j \{ f_j \} \quad . \tag{4.1}$$

In practical applications, the fineness measures f_j and f can be estimated by an inspection of the projection of the target on the reference plane E. The fineness measure depends on the aspect of the target, on the type of the threat and on the type of the vulnerability model. It is, therefore, not a constant for a given three-dimensional target geometry description. However, the order of magnitude of f should be a valid indicator for the smallest diameters of relevant details in a target. An example of f is discussed in Section 7.

The concept of the fineness measure is important for the representation of target components in the vulnerability integral approximations (3.3) and (3.4). If the distances between the sampling points (x_{il},y_{il}) are larger than the fineness measure then relevant components of the target description might not be represented in the integrals. Also, if a cellular sampling point arrangement systematically excludes a set of small components then the standard deviation estimates (3.5) and (3.6) are not valid. Therefore, it is reasonable to require that the average distance between sampling points is smaller than a fraction (for instance, smaller then one half) of the fineness of the target description. On the other hand, there is no advantage to have a computing grid with average distances between sampling points much smaller than the fineness measure.

An average distance between uniformly distributed sampling points in a plane can be defined as follows. Let k sampling points be located in an area A_k. We assign to each point an area A_k/k, represent this area by a circle with the diameter δ, and define δ as the average distance between the points. Explicitly, for given sampling area A_k and number k of sampling points the *average distance* is

$$\delta = \left(\frac{4}{\pi} \cdot \frac{A_k}{k} \right)^{1/2} \quad . \tag{4.2}$$

For instance, if the computing cells are squares with the side length s, and the number of samples per cell is k then the average distance between sampling points is

$$\delta = s\sqrt{4/(\pi k)} = 1.13\, s/\sqrt{k} \quad . \tag{4.3}$$

If the grid is triangular with the side length s_Δ then the corresponding formula is

$$\delta = s_\Delta \sqrt{(2 \sin 60°)/(\pi\ k)} = 0.74\, s_\Delta\, /\sqrt{k} \quad . \tag{4.4}$$

A reasonable value of the average distance between sampling points is

$$\delta \leq \frac{1}{2} f \quad . \tag{4.5}$$

This value might be too large if all nodal areas are square-like or circle-like. On the other hand, real target descriptions characteristically have complicated component projections and the indicated δ should be about right for the capturing of relevant slender nodal areas.

For a square grid, eq. (4.5) can be replaced by

$$s \leq 0.44\, f \sqrt{k} \tag{4.6}$$

or by

$$k \geq 5.1 \left(\frac{s}{f}\right)^2 \quad . \tag{4.7}$$

Eq. (4.6) and (4.7) are conditions that the size of square cells and number of sampling points in each cell are commensurate with the fineness of the target description.

If the integrals are computed by a general Monte Carlo algorithm without a grid pattern then the condition (4.5) in terms of the number k of samples is

$$k \geq \frac{16}{\pi} \frac{S}{f^2} = 5.1 \frac{S}{f^2} \quad , \tag{4.8}$$

where S [m^2] is the sampling area, i.e. the silhouette of the target or the averaging area A.

5. Integration Accuracy Based on Nodal Areas.

In this section we estimate the standard deviation of the discrete approximations of vulnerability integrals for the case where the integrand can be represented in terms of nodal values and nodal areas. First we consider the vulnerable area V_S. By definition,

$$\bar{V}_S - V_S = S \sum_{j=1}^{c} a_j \left(\bar{v}_{Fj} - \frac{V_S}{S}\right) \quad , \tag{5.1}$$

where a_j is the fraction of the nk sampling points that are inside the nodal area F_j. If the number of sampling points is sufficiently large then a_j estimates the probability that a sampling point falls within the nodal area F_j, that is

$$a_j \approx \frac{F_j}{S} \quad , \tag{5.2}$$

and the standard deviation of a_j is (Ref. 1, p. 168)

$$\sigma(a_j) = \left[\frac{1}{nk} \frac{F_j}{S} \left(1 - \frac{F_j}{S}\right) \right]^{1/2} \leq \frac{1}{\sqrt{nk}} \frac{1}{2} \quad . \tag{5.3}$$

Hence the standard deviation of $\bar{V}_S$ is

$$\sigma(\bar{V}_S) = \frac{S}{\sqrt{nk}} \left[\sum_{j=1}^{c} \left(\bar{v}_{Fj} - \frac{V_S}{S} \right)^2 \frac{F_j}{S} \left(1 - \frac{F_j}{S}\right) \right]^{1/2} \quad . \tag{5.4}$$

Estimates of bounds for $\sigma(\bar{V}_S)$ can be obtained by manipulations outlined in the Appendix. The results are

$$\left.\begin{aligned} \sigma(\bar{V}_S) \;&\leq \frac{S}{\sqrt{nk}} \frac{\sqrt{c}}{2} \left[\left(v_{Fj\max} - \frac{V_S}{S} \right) \left(\frac{V_S}{S} - v_{Fj\min} \right) \right]^{1/2} \leq \\ &\leq \frac{S}{2\sqrt{nk}} \frac{\sqrt{c}}{2} \left(v_{Fj\max} - v_{Fj\min} \right) \leq \frac{S}{2\sqrt{nk}} \frac{\sqrt{c}}{2} \quad . \end{aligned}\right\} \tag{5.5}$$

Even the least accurate bound in eq. (5.5) is for $c<4$ smaller than the general bound (3.5). If $c \geq 4$ then eq. (5.4) should produce a better bound than eq. (3.5).

For the average vulnerability V_A we have

$$\bar{V}_A - V_A = \sum_{j=0}^{e} b_j \left(\overline{(\gamma v)}_{Fj} - V_A \right) \approx \sum_{j=0}^{e} \frac{(FA)_j}{A} \left(\overline{(\gamma v)}_{Fj} - V_A \right) \quad , \tag{5.6}$$

where b_j is the fraction of sampling points that are in $(FA)_j = F_j \cap A$, and $(FA)_j/A$ estimates the probability that a random point falls within $(FA)_j$. The standard deviation of the estimate $(FA)_j/A$ is

$$\sigma\left(\frac{(FA)_j}{A} \right) = \frac{1}{\sqrt{mk}} \left[\frac{(FA)_j}{A} \left(1 - \frac{(FA)_j}{A} \right) \right]^{1/2} \quad , \tag{5.7}$$

or, because $n/m = S/A$

$$\sigma\left(\frac{(FA)_j}{A} \right) = \frac{1}{\sqrt{nk}} \frac{\sqrt{S}}{\sqrt{A}} \left[\frac{(FA)_j}{A} \left(1 - \frac{(FA)_j}{A} \right) \right]^{1/2} \quad . \tag{5.8}$$

Hence

$$\sigma(\bar{V}_A) = \frac{1}{\sqrt{nk}} \frac{\sqrt{S}}{\sqrt{A}} \left[\sum_{j=0}^{e} \left(\overline{(\gamma v)}_{Fj} - V_A \right)^2 \frac{(FA)_j}{A} \left(1 - \frac{(FA)_j}{A} \right) \right]^{1/2} \quad . \tag{5.9}$$

Bounds for the standard deviation are in analogy to eq. (5.5)

$$\left.\begin{aligned}\sigma(\bar{V}_A) &\le \frac{1}{\sqrt{nk}}\,\frac{\sqrt{S}}{\sqrt{A}}\,\frac{\sqrt{e+1}}{2}\left[((\overline{\gamma v})_{Fj\max}-V_A)(V_A-(\overline{\gamma v})_{Fj\min})\right]^{1/2} \le \\ &\le \frac{1}{2\sqrt{nk}}\,\frac{\sqrt{S}}{\sqrt{A}}\,\frac{\sqrt{e+1}}{2}\left[(\overline{\gamma v})_{Fj\max}-(\overline{\gamma v})_{Fj\min}\right] \le \\ &\le \frac{1}{2\sqrt{k}}\,\frac{s}{\sqrt{A}}\,\frac{\sqrt{e+1}}{2}\ .\end{aligned}\right\} \qquad (5.10)$$

The accuracy estimates in this section are based on a piecewise-constant nature of the integrand and assume a random distribution of sampling points. We shall see in the next section that one can obtain smaller estimates if also the cellular sampling point arrangement is taken into account. Therefore, if such an arrangement is used and the cell size is commensurate with the target detail then eqs. (5.4) and (5.9) are upper bounds of standard deviations.

6. Integration Accuracy Based on Cells

In this section, we estimate the accuracy of the discrete approximations of the vulnerability integrals in the case where the sampling points are arranged in a cell pattern and the cells are commensurate with the target description.

Let $\bar{v}_i$ be the average value of $v(x,y)$ in the computing cell i. Then the exact value of the vulnerable area integral (2.1) is

$$V_S = C\sum_{i=1}^{n}\bar{v}_i \ . \qquad (6.1)$$

The difference between the approximation (3.3) and V_S is

$$\bar{V}_S - V_S = C\sum_{i=1}^{n}\left[\frac{1}{k}\sum_{l=1}^{k}v_{il}-\bar{v}_i\right] \ . \qquad (6.2)$$

The summation is over all those cells which intersect with the silhouette S. Next, we subdivide the n computing cells into two groups. Let one group consist of $\bar{t}$ cells that do not contain nodal area boundaries, and let the set of the corresponding cell indexes be $\{t\}$. Let the parameters of the other group (cells containing boundaries) be denoted by $\bar{b}$ and $\{b\}$, respectively. Then eq. (6.2) can be reformulated as follows:

$$\bar{V}_S - V_S = C\sum_{i\in\{t\}}\left[\frac{1}{k}\sum_{l=1}^{k}v_{il}-\bar{v}_i\right] + C\sum_{i\in\{b\}}\left[\frac{1}{k}\sum_{l=1}^{k}v_{il}-\bar{v}_i\right] \ . \qquad (6.3)$$

The first sum in eq (6.3) is close to zero because by definition the effect function $v(x,y)$ is about constant within each cell. We assume in the following that the first sum can be neglected.

The second sum in eq. (6.3) is

$$S_b = C \sum_{i \in \{b\}} \left[\frac{1}{k} \sum_{l=1}^{k} v_{il} - \bar{v}_i \right] \quad . \tag{6.4}$$

The summation is over the b cells which contain component boundaries. Let Δv_i be the range of $v(x,y)$ in the cell i. Then $|S_b|$ can be bounded by

$$|S_b| \leq C \sum_{i \in \{b\}} \Delta v_i = s^2 \sum_{i \in \{b\}} \Delta v_i \quad . \tag{6.5}$$

A cellular arrangement of the sampling points has advantages only if the cell size s is small compared to the target description fineness measure f. We therefore assume that commensurability is satisfied by a large margin:

$$s \ll f \quad . \tag{6.6}$$

We now split the sum (6.5) over all boundary cells in partial sums over cells containing the boundary of each nodal area F_j, and over the outer boundary of the integration area S, and estimate the bound of $|S_b|$ by separately bounding each of these partial sums. Let p_{Fj} be the length of the perimeter of F_j, p_S be the length of the outer boundary, Δv_{pFj} be the maximum of the absolute value of the discontinuity of $v(x,y)$ across the boundary of F_j, Δv_{pS} be the maximum absolute value of the discontinuity across the outer boundary, and Δv_p be the maximum absolute value of all discontinuities:

$$\Delta v_p = \max_i \{ \Delta v_i \} \quad . \tag{6.7}$$

Let p_Σ be the total length of all boundaries within the integration area:

$$p_\Sigma = \frac{1}{2} \left(\sum_{j=1}^{c} p_{Fj} + p_S \right) \quad . \tag{6.8}$$

The discretization error (6.3) of the vulnerable area is equal to the absolute value of S_b and can be bounded by

$$|\bar{V}_S - V_S| \leq s^2 \sum_{i \in \{b\}} \Delta v_i \leq \frac{s}{2} \left(\sum_{j=1}^{c} p_{Fj} \Delta v_{pFj} + p_S \Delta v_{pS} \right) \tag{6.9}$$

and furthermore by

$$|\bar{V}_S - V_S| \leq s \, p_\Sigma \Delta v_p \leq s \, p_\Sigma \quad . \tag{6.10}$$

An estimate for the perimeter p_{Fj} is

$$p_{Fj} \approx 2 \frac{F_j}{f_j} \left(1 + \frac{f_j^2}{F_j} \right) \quad . \tag{6.11}$$

The formula (6.11) is about right for slender F_j and might be used if the perimeter p_{Fj} is not available. However, in general estimates of the p_{Fj} can be easily determined by an inspection of the target description.

In a single boundary cell, an estimated bound for the standard deviation of the discretization is (see Appendix)

$$\sigma(S_{bi}) \le C \frac{1}{\sqrt{k}} \frac{1}{2} \Delta v_i = \frac{s^2}{\sqrt{k}} \frac{1}{2} \Delta v_i \ . \tag{6.12}$$

The corresponding estimate of the standard deviations of S_b and $\bar{V}_S$ is

$$\sigma(\bar{V}_S) = \sigma(S_b) \le \frac{s^2}{2\sqrt{k}} \left(\sum_{i \in \{b\}} (\Delta v_i)^2 \right)^{1/2} , \tag{6.13}$$

or

$$\sigma(\bar{V}_S) = \frac{s^{3/2}}{2\sqrt{2k}} \left(\sum_{j=1}^{c} p_{Fj} (\Delta v_{pFj})^2 + p_S (\Delta v_{pS})^2 \right)^{1/2} \le \frac{s^{3/2} (p_\Sigma)^{1/2}}{2\sqrt{k}} \Delta v_p \ . \tag{6.14}$$

Eqs. (6.13) and (6.14) are alternatives to eqs. (5.4) and (5.5). In order to compare both sets of formulas we use the relation $s \approx \sqrt{S/n}$ and obtain

$$\sigma(\bar{V}_S) \le \frac{s^{3/2} (p_\Sigma)^{1/2}}{2\sqrt{k}} \Delta v_p = \frac{1}{n^{1/4}\sqrt{nk}} \frac{S^{3/4} (p_\Sigma)^{1/2}}{2} \Delta v_p \ . \tag{6.15}$$

Thus, for sufficiently large n the estimates (6.13) or (6.14) are smaller than the estimates (5.4) or (5.5) that do not take into account the cellular arrangement of sampling points.

We now consider the average vulnerability integral (2.5). Let its exact value be

$$V_A = \frac{C}{A} \sum_{i=1}^{m} \overline{(\gamma v)}_i \ , \tag{6.16}$$

where the summation is over the m cells that intersect with A. The difference between the discretization (3.4) and V_A is

$$\bar{V}_A - V_A = \frac{C}{A} \sum_{i=1}^{m} \left(\frac{1}{k} \sum_{l=1}^{k} (\gamma v)_{il} - \overline{(\gamma v)}_i \right) = \frac{1}{m} \sum_{i=1}^{m} \left(\frac{1}{k} \sum_{l=1}^{k} (\gamma v)_{il} - \overline{(\gamma v)}_i \right) . \tag{6.17}$$

Within each computing cell the difference is bounded by

$$| \bar{V}_A - V_A |_i \le \frac{1}{m} (\bar{v}_i \Delta\gamma_i + \bar{\gamma}_i \Delta v_i) \ , \tag{6.18}$$

where $\bar{v}_i$ and $\bar{\gamma}_i$ are average values of $v(x,y)$ and $\gamma(x,y)$, respectively, in the cell i, and Δv_i and $\Delta\gamma_i$ are the corresponding variations. Let $\{A\}$ be the set of cell indexes of cells that

intersect with A. The first term in eq. (6.18) provides the sum

$$D_{1A} = \frac{C}{A} \sum_{i=1}^{m} \bar{\nu}_i \, \Delta\gamma_i = \frac{1}{m} \sum_{i=1}^{m} \bar{\nu}_i \, \Delta\gamma_i \leq \max_{i \in \{A\}} [\bar{\nu}_i \, \Delta\gamma_i] \ . \tag{6.19}$$

The second term in eq. (6.18) contributes nothing if the cell is inside a nodal area. For cells containing nodal boundaries, we can estimate the total contribution to the difference $\bar{V}_A - V_A$ by using the same steps as for the accuracy estimates of $\bar{V}_S$. The only important difference is that all perimeter lengths and maxima pertain to the averaging area A instead of S. We indicate this by placing a tilde over the corresponding symbols. The result is

$$D_{2A} = \frac{C}{A} \sum_{i=1}^{m} \bar{\gamma}_i \, \Delta\nu_i \leq \frac{s}{2A} \left(\sum_{j=0}^{e} \tilde{p}_{Fj} \, \gamma_{pFj} \, \Delta\tilde{\nu}_{pFj} + p_A \, \gamma_{pA} \, \Delta\nu_{pA} \right) , \tag{6.20}$$

where γ_{pFj} and γ_{pA} are the largest values of $\gamma(x,y)$ on the boundaries p_{Fj} and p_A, respectively. Eq. (6.20) can be bounded further by

$$D_{2A} \leq \frac{s}{A} \, p_{\Sigma A} \, \gamma_p \, \Delta\tilde{\nu}_p \leq \frac{s}{A} \, \gamma_p \, p_{\Sigma A} \ , \tag{6.21}$$

where $p_{\Sigma A}$ is the total length of boundaries within A and γ_p is the largest value of $\gamma(x,y)$ on all boundaries. Combining the estimates D_{1A} and D_{2A} one obtains, for instance the bound

$$| \bar{V}_A - V_A | \leq \max_{i \in \{A\}} [\nu_i \, \Delta\gamma_i] + \frac{s \, p_{\Sigma A}}{A} \, \gamma_p \, \Delta\tilde{\nu}_p \tag{6.22}$$

or some similar expression based on some of the forms of D_{1A} and D_{2A}. In order to expose the trend of the estimate, we introduce the quantity γ' by the definition

$$\gamma_i' = \frac{\Delta\gamma_i}{s} \ . \tag{6.23}$$

For linear $\gamma(x,y)$ it approximates the absolute value of the gradient of γ in the cell i. Then eq. (6.22) can be reformulated as follows

$$| \bar{V}_A - V_A | \leq s \left(\max_{i \in \{A\}} [\bar{\nu}_i \, \gamma_i'] + \frac{p_{\Sigma A}}{A} \, \gamma_p \, \Delta\tilde{\nu}_p \right) , \tag{6.24}$$

which shows that the estimate of the difference is proportional to the cell size s.

To obtain the standard deviation of $\bar{V}_A$ we follow the same steps as for the derivation of eqs. (6.12) through (6.15). The result can be formulated by

$$\sigma(\bar{V}_A) \leq \left(\frac{1}{k} \frac{C}{A} \max_{i \in \{A\}} [\bar{\nu}_i \, \Delta\gamma_i]^2 + \frac{s^3 \, p_{\Sigma A}}{4k} \frac{1}{A^2} (\gamma_p \, \Delta\tilde{\nu}_p)^2 \right)^{1/2} , \tag{6.25}$$

or in one of the following equivalent forms

$$\sigma(\bar{V}_A) \le \frac{s}{\sqrt{k}\sqrt{A}} \left(\max_{i\in\{A\}} [\bar{\nu}_i \Delta\gamma_i]^2 + \frac{s\, p_{\Sigma A}}{4A} (\gamma_p \Delta\tilde{\nu}_p)^2 \right)^{1/2}, \tag{6.26}$$

$$\sigma(\bar{V}_A) \le \frac{1}{n^{1/4}\sqrt{nk}} \left(\frac{S}{A}\right)^{3/4} \left(\frac{\sqrt{SA}}{\sqrt{n}} \max_{i\in\{A\}} [\bar{\nu}_i \gamma_i']^2 + \frac{p_{\Sigma A}}{4\sqrt{A}} (\gamma_p \Delta\tilde{\nu}_p)^2 \right)^{1/2}. \tag{6.27}$$

The estimate (6.27) is smaller than (5.10) if n is sufficiently large.

The estimates in this section presuppose small cell sizes ($s \ll f$) whereas the estimates in Section 5 depend only on the number of samples. If the sample number n is increased then eventually the estimates in this section become better (smaller) than those of Section 5. If n is not very large then the estimates of Section 5 might be smaller. If there is a difference then in general one should use the smaller estimate. The estimates at the end of Section 3 are most conservative, because they do not postulate any properties of the integrand or sampling point arrangement. On the other hand, they are very simple to calculate and might be the only practical formulas if the target description is complicated.

7. Application Example

In the previous sections we have derived a number of accuracy estimates and criterions for a rational choice of the numerical integration method and of the level of detail in target description. In this section we illustrate the application of these results with a simple artificial example. We have chosen an artificial example to have a clear presentation of the principal aspects of the criterions. In a real life example one would have to discuss the possibly complicated details of the target. Such discussions are necessarily lengthy and do not contribute to the understanding of the method.

Table 1. Sizes and Vulnerabilities of Nodal Areas.

j	F [m^2]	p [m]	f [m]	$\bar{\nu}$	$\delta\nu$
1	3.00	11.00	0.5	0.05	0.05
2	1.57	5.14	0.8	1.0	0.0
3	1.10	4.20	1.0	0.8	0.05
4	5.33	19.34	0.15	0.4	0.05
5	1.00	40.0	0.05	1.0	0.0
2†	2.57	45.14	0.05	1.0	0.0
4†	4.33	59.34	0.15	0.4	0.05

$S = A = 11$ m^2, $p_S = 15$ m,
$p_\Sigma = 27.34$ m, $f = f_4 = 0.15$ m,
$p_{\Sigma\dagger} = 67.34$ m, $f_\dagger = f_{2\dagger} = 0.05$ m.

Figure 2 shows the projection of a target description onto the reference plane. The corresponding numerical data are listed in Table 1. We shall use these data to compute the

average vulnerability whereby the averaging is over the whole silhouette. (Hence, $A=S$ and $\gamma=1$). The first four entries in the table contain the parameters of the four nodal areas shown in Figure 2. The last three entries we shall discuss later. Using the data for $j=1,\ldots,4$ we compute with eqs. (2.13) and (2.14) the average vulnerability V_A of the target consisting of the first four components

$$V_A = 0.430 \ , \tag{7.1}$$

and the corresponding intrinsic spread D_A of V_A:

$$D_A = 0.043 \ . \tag{7.2}$$

The commensurate average distance between sampling points equals 0.075 m according to eq. (4.5). If a square grid is used with one sampling point per cell then the side length of the cell should be less than 0.06 m (see eq. (4.6)). If the side length is 0.1 m then, according to eq. (4.7), one should take two samples from each cell. However, the criterions based on the target fineness measure implicitly assume that the fineness is typical for the target description and that the nodal fineness measures are diameters of relevant areas. In the present example, the fineness is determined by the width of the isthmus between the nodal areas F_2 and F_3. It is obvious that a failure to represent the isthmus in the vulnerability integral would not significantly affect the average vulnerability. Therefore, a better value for the fineness measure is $f=0.5$ m which approximately represents typical diameters of the narrow parts of the nodal areas if the isthmus between F_2 and F_3 is neglected. Then the commensurate cell size according to eq. (4.6) should be less than 0.2 m, that is, a cell size of 0.1 m is adequate.

We test the relevance of the isthmus by using eq. (2.15) and assuming that the area of the isthmus is added to F_2. (Adding to F_3 has a smaller effect). The effect of this replacement on the average vulnerability is less than

$$T \, \frac{1}{A} \, (\, v_2 - v_4 \,) \approx (0.15 \cdot 0.5) \cdot \frac{1}{11} \cdot 0.6 = 0.0041 \ , \tag{7.3}$$

which is much smaller than the intrinsic error D_A of V_A.

Let the cell size for the numerical integration be $s=0.1$ m, and let the number of samples from each cell be $k=1$. Then the estimate (3.6) for the standard deviation of the numerically computed average vulnerability $\bar{V}_A$ from the true value V_A is

$$\sigma(\bar{V}_A) \le \frac{s}{\sqrt{A}} \left[(\Gamma - V_A) \, V_A \right]^{1/2} = \frac{0.1 \cdot \sqrt{0.570 \cdot 0.430}}{\sqrt{11}} = 0.0172 \tag{7.4}$$

which is about 40% of the intrinsic error D_A. More accurate are the estimates (5.9) and (6.26). With eq. (5.9) we obtain

$$\sigma(\bar{V}_A) = \frac{1}{\sqrt{nk}} \left[\sum_{j=1}^{4} (\bar{v}_j - V_A)^2 \frac{F_j}{A} \left(1 - \frac{F_j}{A} \right) \right]^{1/2} = \frac{0.2845}{\sqrt{nk}} = 0.0858 \cdot s \ , \tag{7.5}$$

where we have used the relation $\sqrt{n}=\sqrt{S}/s=\sqrt{11}/s$. This estimate shows that an integration with the cell size $s=0.1$ m is adequate because the standard deviation of the numerical integration is only about 20% of the intrinsic error D_A of the average vulnerability, eq. (7.2). Even a cell size $s=0.2$ m is sufficiently accurate in this example and would require only a fourth of the computing time.

The first term in the standard deviation estimate formula (6.26) equals zero, because in our example γ is constant and $\Delta\gamma_i=0$. The second term yields for $s=0.1$

$$\sigma(\bar{V}_A) \le \frac{s^{3/2}\,(p_\Sigma)^{1/2}}{\sqrt{k}\;2\;A}\,\Delta v_p = \frac{s^{3/2}\,\sqrt{27.34}}{2\cdot 11}\cdot 0.75 = 0.1782\cdot s^{3/2} = 0.0056\ . \qquad (7.6)$$

Thus, the more accurate formulas yield in this example estimates that are smaller than the general estimate (7.4) by a factor of 0.5 to 0.3.

The *bound* of the error of the numerical integration can be computed using eq. (6.22):

$$|\,\bar{V}_A - V_A\,| \le \frac{s\cdot p_\Sigma}{A}\cdot\Delta v_p = \frac{s\cdot 27.34}{11}\cdot 0.75 = 1.864\cdot s\ . \qquad (7.7)$$

The more accurate eq. (6.20) produces

$$|\,\bar{V}_A - V_A\,| \le \frac{s}{2\,A}\left(\sum_{j=1}^{4} p_{Fj}\Delta v_{pFj} + p_S\Delta v_{pS}\right) = \frac{s}{22}\cdot 27.688 = 1.258\cdot s\ . \qquad (7.8)$$

For $s=0.1$ we obtain a bound that is three times as large as the intrinsic error D_A of V_A. Therefore, if guaranteed error bounds are important then the cell size s should be about 0.03 m. However, because the best estimate of the standard deviation of $\bar{V}_A$ is only about 13% of the intrinsic error D_A, the large estimate of the bound likely is too pessimistic and can be ignored.

We now assume that the target contains in addition to the first four components a very sensitive fifth component with a small diameter (e.g., a fuel line), and determine whether that component should be included in the target description. Let the effective diameter of the component be 2 cm, its length be 10 m, and let it be located in the component area 4. The presented length of the line is rather large: it is two times as long as the horizontal dimension of the silhouette and about three times as long as the length of the area $j=4$. We use eq. (2.15) and estimate the effect of the additional component on the average vulnerability. The presented area of the component is $T_5=0.02\cdot 10=0.2$ m^2 and

$$T_5\cdot\frac{1}{A}\cdot(v_5-v_4) = 0.2\cdot\frac{1}{11}\cdot 0.6 = 0.011\ . \qquad (7.9)$$

This is about one fourth of the intrinsic error. Therefore, the component is not relevant and the inclusion of such a component in the target description is a waste of resources. On the other hand, if such a component is already present in the target description, then it can be ignored in the sense that the cell size need not be made commensurate with the fineness measure of the component.

To have an example where a change of the target description is indicated we assume that the additional fuel line has an effective diameter of 5 cm and a length of 20 m. It is listed as the fifth component in the Table 1. Its effect equals 0.055 and is about the same as the intrinsic error, eq. (7.2). (Also, the effective presented area of the line is formidable: it is about the same as the area F_3 or about 10% of the silhouette). Because the fifth component is assumed to be located in the nodal area $j=4$, the area and its perimeter must be modified. We assume for simplicity that the fineness measure f_4 is not changed, and list the other new parameters of F_4 in the line $j=4\dagger$ of Table 1. Because $v_5=v_2$, the new component belongs to the nodal area F_2 the parameters of which are changed and listed in the line $j=2\dagger$. Finally, the total length of nodal area boundaries p_Σ is increased to $p_{\Sigma\dagger}$ and the new fineness measure of the target description is $f_\dagger=f_5=f_{2\dagger}$. The new table of the target description now consists of the entries $j=1$, $2\dagger$, 3 and $4\dagger$.

Using the modified table, one obtains for the average vulnerability

$$V_{A\dagger} = 0.485 . \tag{7.10}$$

Hence, by adding the fuel line to the target description the average vulnerability is increased by 0.055. The intrinsic spread of the new result is

$$D_{A\dagger} = 0.038 . \tag{7.11}$$

The spread $D_{A\dagger}$ is smaller than D_A, because the added component has an error free effect function value $v_5=1$.

The standard deviation of $\bar{V}_{A\dagger}$ is, if computed with eqs. (3.6), (5.9) or (6.26), respectively,

$$\sigma(\bar{V}_{A\dagger}) = \frac{0.1\cdot\sqrt{0.515\cdot 0.485}}{\sqrt{11}} = 0.0151 , \tag{7.12}$$

$$\sigma(\bar{V}_{A\dagger}) = \frac{0.3093}{\sqrt{nk}} = \frac{0.0933}{\sqrt{k}}\cdot s = 0.0093 , \tag{7.13}$$

$$\sigma(\bar{V}_{A\dagger}) \le \frac{s^{3/2}\cdot\sqrt{67.34}}{\sqrt{k}\ 2\cdot 11}\cdot 0.75 = 0.2798\cdot s^{3/2} = 0.0088 . \tag{7.14}$$

Thus, the cell size $s=0.1$ m is adequate for the modified target in the sense that the result of the numerical integration likely will be within the intrinsic spread of the average vulnerability, and that the standard deviation of the integral is less than 20% of the vulnerability increase 0.055 due to the new component.

Next we compute estimates for the bound of the difference between $\bar{V}_{A\dagger}$ and $V_{A\dagger}$. Using eq. (6.22) one obtains

$$|\bar{V}_{A\dagger} - V_{A\dagger}| \le \frac{s\cdot 67.34}{11}\cdot 0.75 = 4.591\cdot s , \tag{7.15}$$

and, with the more accurate eq. (6.20),

$$| \bar{V}_{At} - V_{At} | \leq 3.440 \cdot s \ . \qquad (7.16)$$

Therefore, to *guarantee* a numerical integration accuracy better than the effect of the fifth component one needs a cell size of about 0.055/3.440=0.016 m. This is about the same as the commensurate cell size which is 0.020 m according to eq. (4.6). For the cell size 0.02 m, the number of cells is about 25 times larger than for $s=0.10$ m. We note in passing that sampling of 25 random points per cell results in the same increase of computing time and a substantial reduction of the standard deviation estimate but does not guarantee that the effect of the fifth component is correctly computed, because the random sampling points might not fall within the projection of the component.

In summary, a cell size of 0.1 m with one random sample per cell is adequate for the computation of the average vulnerability. Likely even the effect of the (long and thick) fuel line (the fifth component) will be correctly determined. However, because the commensurability condition is not satisfied a detection of the effect of the fifth component is not guaranteed. If a guaranteed computation of that effect is important then the cell size must be reduced at the cost of a corresponding increase of the computing time by a factor of 25 or more.

Finally, the example illustrates the tediousness of the application of the theoretically better formulas for error estimates. Usually, the simple standard deviation estimate, eq. (7.4) or (7.12), will suffice to establish adequacy of the numerical integration, and a detailed analysis of the target description will not be necessary. The significance of the more accurate formulas is mainly theoretical, showing that a cellular point arrangement is indeed better than random sampling.

8. Summary and Conclusions

We considered in this report the computation of target system vulnerabilities by numerical integration of local effect functions over a reference plane. Accuracy is affected by three sources of errors: an "intrinsic" error caused by inaccurate models of component response, an error caused by inadequate target geometry description and a numerical integration error. In a reasonable algorithm the magnitudes of these three errors should be of the same order, because the final accuracy is dominated by the largest error and a reduction or elimination of one or both of the smaller errors does not change the order of magnitude of the total error. In this report, we assume as given the "intrinsic" error which is determined by the accuracies of component vulnerabilities. Errors from the other two sources can be controlled by proper choices of target description detail and numerical integration procedures, respectively. Error estimates provided in this report help one to make such choices.

We assume that the integration is done with a Monte Carlo method as follows. First, the integration area is overlaid with a computing net consisting of square cells with the cell side lengths $s=0.1$ m. Next, the integrand is computed at k random sampling points in each computing cell, and the integral is obtained by weighted adding of the sampled integrand

values. The usual computation is done with $k=1$ sampling points from each computing cell.

The following particular aspects might be treated based on the results presented in this report:

(a) Estimates and bounds of the overall accuracy of vulnerability calculations.
(b) Relevance of particular components.
(c) Rational choice of computing mesh based either on the fineness of the target description or on the achievable accuracy.

Formulas which may be used to address these problems are listed in Table 2 by application area.

Table 2. Numbers of Formulas by Application.

Application	Vulnerable area	Average vulnerability
Intrinsic error	(2.8), (2.10)	(2.12), (2.14)
Standard deviation of integral	(3.5), (5.4), (5.5), (6.13), (6.14), (6.15)	(3.6), (5.9), (5.10), (6.25), (6.26), (6.27)
Bounds of integration error	(6.5), (6.9), (6.10)	(6.19), (6.20), (6.22), (6.24)
Component relevance	(2.11)	(2.15)
Commensurate mesh size	(4.6)	

Three general conclusions can be drawn from the discussions in this report. First, a statement about the computing cell size. The standard deviation of the Monte Carlo computation of the vulnerability averaged over the silhouette is (see eq. (3.6))

$$\sigma(\bar{V}_A) \leq \frac{1}{2}\frac{s}{\sqrt{S}} \quad .$$

Assuming $S=10$ m^2 as typical for the order of magnitude of an armored vehicle silhouette, and setting $s=0.1$, one obtains

$$\sigma(\bar{V}_A) \leq 0.16 \cdot s = 0.016 \quad .$$

Hence, for a cell size of $s=0.1$ m the standard deviation of the integral is of the order of the second digit of the average vulnerability. This is likely less than the intrinsic error of the average vulnerability V_A due to model inaccuracies and, therefore, a cell size of 0.1 m is adequate for the computation of directional average vulnerability of a typical tank.

The second conclusion pertains to the importance of detail in the target description. Minute details are necessary if one wants to predict the effect of a single shot on a particular target. For any average vulnerability which is defined by an integral over an area

in the reference plane, the contribution of a detail is directly proportional to the relative size of its presented area. If the intrinsic inaccuracy of the average vulnerability indicator is of the order of 5%−10%, a typical value, then any detail with an effective presented area of less than 10% of the averaging area is suspect of not being relevant. (The effective presented area is defined as that part of the reference plane where the threat has an effect on the component, see page 7). Such a detail might be removed from the target description without penalty as shown in the example in Section 7. However, the removal should be judicious, because a combination of several irrelevant components might well be relevant. On the other hand, if one wants to investigate the effect of a small detail of the target by comparing the values of the corresponding vulnerability integrals, then the mesh size must be commensurate with the detail. (A simple increase of the number k of points per cell does not guarantee that the effect of a detail is correctly computed). This can increase the computing times by orders of magnitude unless the algorithm is arranged such that a fine net is used only in the area of the detail.

Finally, for a piecewise constant integrand, cellular arrangements of sampling points theoretically yield more accurate results than random sampling if the ceil size is much smaller than the fineness of the target description.

LIST OF REFERENCES

1. Thomas H. Wonnacott and Ronald J. Wonnacott, *Introductory Statistics*, Third Edition, John Wiley & Sons, New York, NY, 1977.

2. Paul H. Deitz and Aivars Ozolins, "Computer Simulations of the Abrams Live-Fire Field Testing", Ballistic Research Laboratory Memorandum Report BRL-MR-3755, May 1989, AD# A209509.

LIST OF SYMBOLS

A – area of averaging in the reference plane E, m^2,
$\{A\}$ – set of cell indexes of cells intersecting with A,
a_j – fraction of sampling points in the nodal area F_j, dimensionless,
$\{b\}$ – set of cell indexes of cells containing boundaries of nodal areas,
$\bar{b}$ – cardinality of $\{b\}$, dimensionless,
C – cell size in computing grid, m^2,
c – number of nodal areas within the silhouette S, dimensionless,
D_A – bound of δV_A, dimensionless,
D_S – bound of δV_S, m^2,
E – reference plane normal to the direction of threat,
e – number of nodal areas within the averaging area A, dimensionless,
F_j – nodal area j, m^2,
$(FA)_j$ – intersection of F_j with A, m^2,
f – fineness of the target description, m,
f_j – fineness of the description of the nodal area F_j, m,
$g(x,y)$ – density of averaging weight, m^{-2},
k – number of samples in a computing cell, dimensionless,
m – number of cells intersecting with the averaging area A, dimensionless,
n – number of cells intersecting with the silhouette S, dimensionless,
p_Σ – total length of boundaries within the silhouette S, m,
$p_{\Sigma A}$ – total length of boundaries within the averaging area A, m,
p_A – perimeter of the averaging area A, m,
p_{Fj} – perimeter of the nodal area F_j, m,
p_S – perimeter of the silhouette S, m,
S – area of target silhouette in the reference plane E, m^2,
s – side length of a square cell in a computing grid, m,
T_j – effective presented area of a target component, m^2,
$\{t\}$ – set of cell indexes of cells completely inside a nodal area,
$\bar{t}$ – cardinality of $\{t\}$, dimensionless,
V_A – average vulnerability, dimensionless,
$\bar{V}_A$ – approximate average vulnerability, dimensionless,
δV_A – bound of error of V_A due to error of $v(x,y)$, dimensionless,
V_S – vulnerable area, m^2,
$\bar{V}_S$ – approximate vulnerable area, m^2,
δV_S – bound of error of V_S due to error of $v(x,y)$, m^2,
$v(x,y)$ – effect of a threat impinging at (x,y), dimensionless,
v_{il} – sample $v(x_{il},y_{il})$, dimensionless,
$\bar{v}_{Fj}$ – nodal (average) value of $v(x,y)$ in the nodal area F_j, dimensionless,
$\bar{v}_{Tj}$ – average value of $v(x,y)$ in the effective area T_j, dimensionless,

$\bar{v}_i$ – average value of $v(x,y)$ in cell i, dimensionless,
$\bar{v}_{0j}$ – average value of $v(x,y)$ in T_j without the component, dimensionless,
Δv_i – discontinuity of $v(x,y)$ in cell i, dimensionless,
Δv_p – maximum discontinuity of $v(x,y)$, dimensionless,
$\Delta \bar{v}_p$ – maximum discontinuity of $v(x,y)$ in A, dimensionless,
Δv_{pA} – maximum discontinuity of $v(x,y)$ on p_A, dimensionless,
Δv_{pFj} – maximum discontinuity of $v(x,y)$ on p_{Fj}, dimensionless,
$\Delta \bar{v}_{pFj}$ – maximum discontinuity of $v(x,y)$ on p_{Fj} in A, dimensionless,
Δv_{pS} – maximum discontinuity of $v(x,y)$ on p_S, dimensionless,
$\delta v(x,y)$ – error bound of $v(x,y)$, dimensionless,
δv_{Fjmax} – maximum value of $\delta v(x,y)$ in F_j, dimensionless,
δv_{Tjmax} – maximum value of $\delta v(x,y)$ in T_j, dimensionless,
x,y – Cartesian coordinates in the reference plane E, m,
Γ – largest value of $\gamma(x,y)$ within $A \cap S$, dimensionless,
$\gamma(x,y)$ – normalized density of averaging weight, dimensionless,
γ_p – maximum of $\gamma(x,y)$ on nodal boundaries, dimensionless,
γ_{ij} – sample $\gamma(x_{ij},y_{ij})$, dimensionless,
γ_p – maximum $\gamma(x,y)$ on the outer boundary, dimensionless,
γ_{pA} – maximum $\gamma(x,y)$ on the perimeter p_A, dimensionless,
γ_{pFj} – maximum $\gamma(x,y)$ on the perimeter p_{Fj}, dimensionless,
γ_{pS} – maximum $\gamma(x,y)$ on the perimeter p_S, dimensionless,
$\Delta\gamma_i$ – absolute variation of $\gamma(x,y)$ in cell i, dimensionless,
$\overline{(\gamma v)}_i$ – average value of $\gamma(x,y)v(x,y)$ in cell i, dimensionless,
$\overline{(\gamma v)}_{Fj}$ – average value of $\gamma(x,y)v(x,y)$ in the nodal area F_j, dimensionless,
$\overline{(\gamma v)}_{Tj}$ – average value of $\gamma(x,y)v(x,y)$ in the component area T_j, dimensionless,
$\overline{(\gamma v)}_{0j}$ – average value of (γv) in area T_j, without the component, dimensionless,
$[\gamma\delta v]_{Fjmax}$ – maximum value of $[\gamma\delta v]$ in F_j, dimensionless,
$[\gamma\delta v]_{Tjmax}$ – maximum value of $[\gamma\delta v]$ in T_j, dimensionless,
γ_i' – approximate $|\text{grad } \gamma|$ in the cell i, 1/m,
δ – average distance between sampling points, m,
$\sigma(\bar{V}_A)$ – estimated standard deviation of $\bar{V}_A$, dimensionless,
$\sigma(\bar{V}_S)$ – estimated standard deviation of $\bar{V}_S$, m^2.

Appendix. Estimate of Monte Carlo Standard Deviation.

Let $h(x)$ be integrable over the x-interval $[a,b]$, and let it have the range $[h_{min},h_{max}]$. Let

$$\bar{h} = \frac{1}{b-a}\int_a^b h(x)\,dx \quad . \tag{A.1}$$

We estimate $\bar{h}$ by chosing k random points $x_j \epsilon [a,b]$ and computing the sample mean

$$H_k = \frac{1}{k}\sum_{j=1}^{k} h(x_j) \quad . \tag{A.2}$$

The expected value of H_k is $\bar{h}$ and an estimate of the variance of the sample mean H_k is (Ref. 1, p. 147)

$$\left.\begin{aligned} \mathrm{Var}(H_k) &= \frac{1}{k^2}\sum_{j=1}^{k}\mathrm{Var}\big(h(x_j)\big) = \frac{1}{k^2}\sum_{j=1}^{k}\big(h(x_j)-H_k\big)^2 = \\ &= \frac{1}{k^2}\sum_{j=1}^{k}h^2(x_j) - \frac{1}{k}H_k^2 = \\ &= \frac{1}{k^2}\sum_{j=1}^{k}\big(h(x_j)-h_{min}\big)^2 - \frac{1}{k}\big(H_k-h_{min}\big)^2 \quad . \end{aligned}\right\} \tag{A.3}$$

A simple upper bound of $\mathrm{Var}(H_k)$ is obtained by taking the largest term in the sum:

$$\mathrm{Var}(H_k) \le \frac{1}{k}\max_j\,[h(x_j)-H_k]^2 \le \frac{1}{k}\max\left\{\,(h_{max}-H_k)^2,\,(H_k-h_{min})^2\,\right\} \quad . \tag{A.4}$$

A generally more accurate bound is

$$\left.\begin{aligned} U &= \frac{1}{k}\,(h_{max}-H_k)\,(H_k-h_{min}) = \\ &= \frac{1}{k}(h_{max}-h_{min})\,(H_k-h_{min}) - \frac{1}{k}(H_k-h_{min})^2 = \\ &= \frac{1}{k^2}\sum_{j=1}^{k}(h(x_j)-h_{min})(h_{max}-h_{min}) - \frac{1}{k}(H_k-h_{min})^2 \quad . \end{aligned}\right\} \tag{A.5}$$

To show that U is an upper bound of $\mathrm{Var}(H_k)$ we compute the difference

$$D = \mathrm{Var}(H_k) - U = \frac{1}{k^2}\sum_{j=1}^{k}\Big[(h(x_j)-h_{min})^2 - (h(x_j)-h_{min})(h_{max}-h_{min})\Big] \quad . \tag{A.6}$$

Eq. (A.6) shows that D is in general negative and vanishes only if the range of $h(x)$ is

restricted to the set $\{h_{min},h_{max}\}$. Therefore,

$$\mathrm{Var}(H_k) \le \frac{1}{k}\,(h_{max}-H_k)(H_k-h_{min}) \le \frac{1}{k}\,\frac{1}{4}\,(h_{max}-h_{min})^2 \quad , \tag{A.7}$$

since H_k can only have values within the interval $[h_{min},h_{max}]$.

The standard deviation of a Monte Carlo calculation thus can be estimated using eq. (A.4) by

$$\sigma(H_k) \le \frac{1}{\sqrt{k}}\,\max\{\,h_{max}-H_k,\,H_k-h_{min}\,\} \le \frac{1}{\sqrt{k}}(h_{max}-h_{min}) \quad , \tag{A.8}$$

or, using the more accurate bound (A.7) by

$$\sigma(H_k) \le \frac{1}{\sqrt{k}}\,\left((h_{max}-H_k)(H_k-h_{min})\right)^{1/2} \le \frac{1}{\sqrt{k}}\,\frac{1}{2}\,(h_{max}-h_{min}) \quad . \tag{A.9}$$

These formulas are not restricted to integration in one dimension, because we have only assumed integrability and used the maximum and minimum properties of $h(x)$. Therefore, the same formulas apply to the calculation of integrals in any dimension, in particular to the surface integrals in vulnerability analysis.

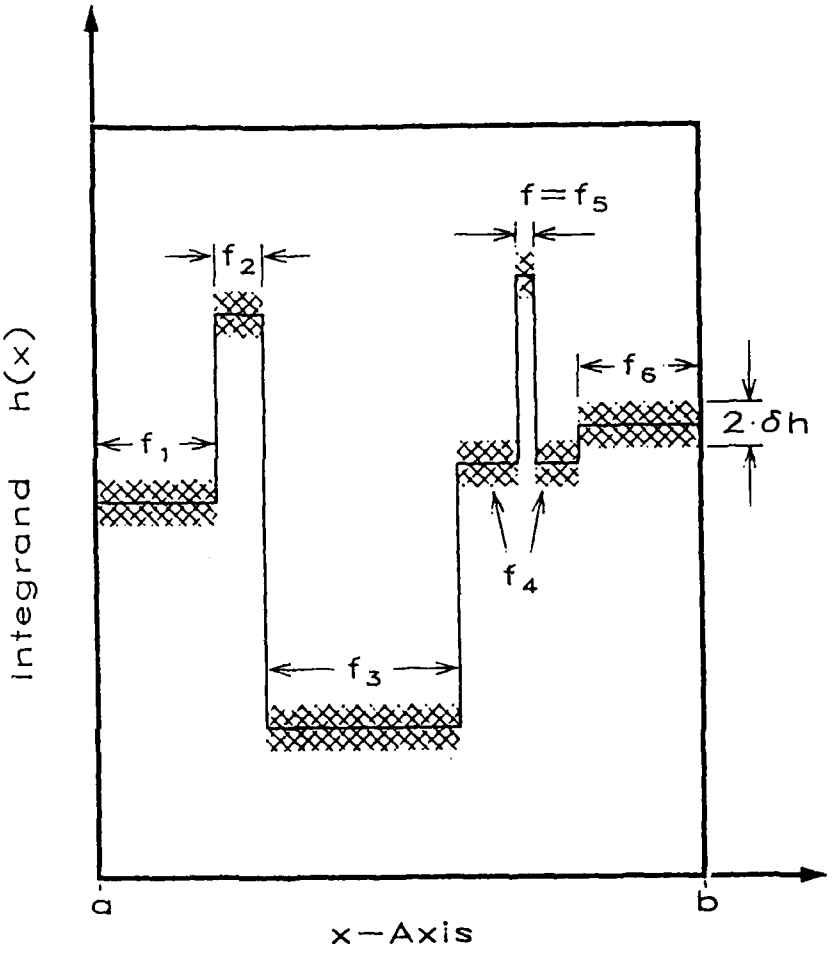

Figure 1. Integration in 1—D

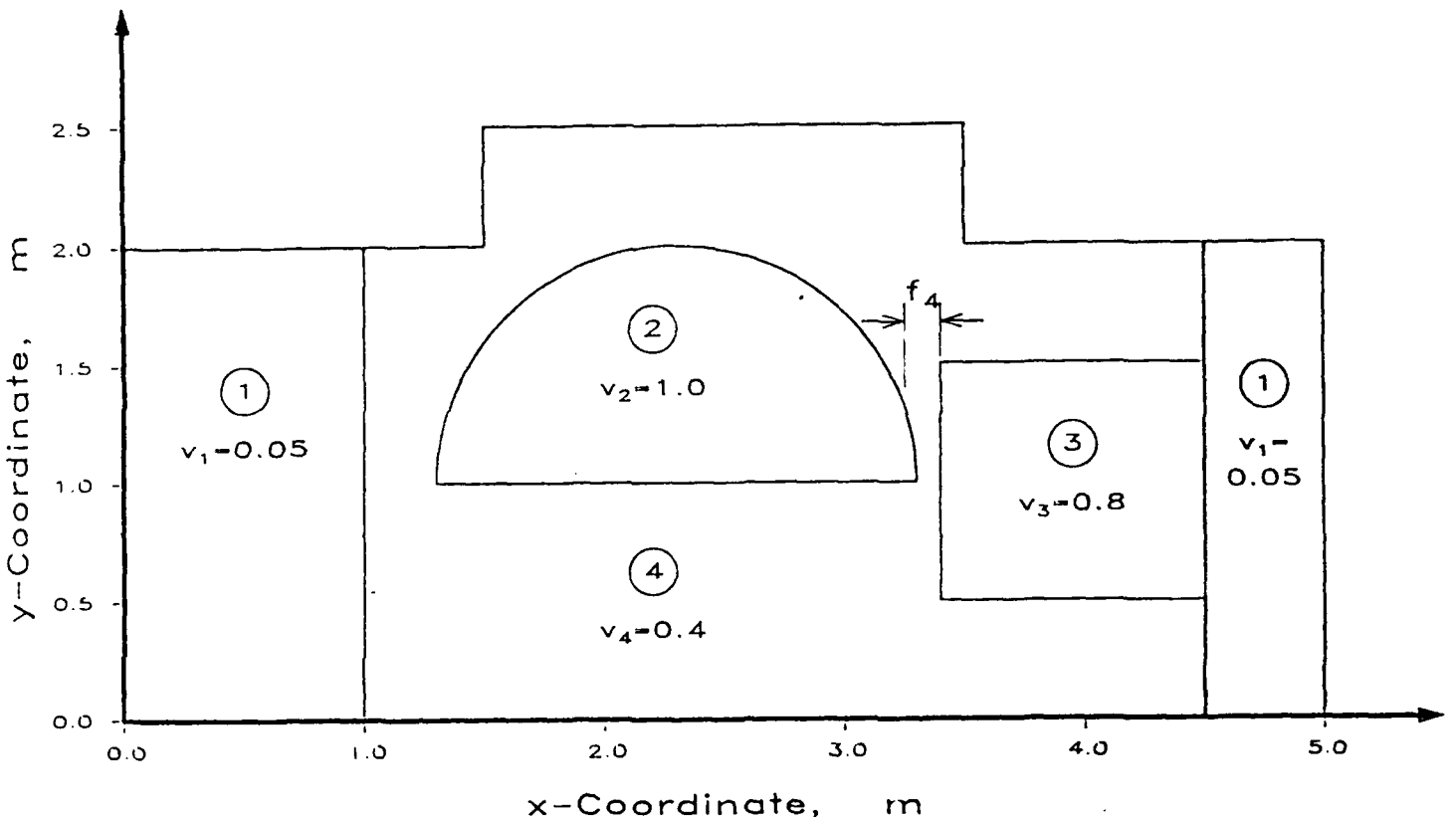

Figure 2. Target projection on the reference plane

No of Copies	Organization
1	Office of the Secretary of Defense OUSD(A) Director, Live Fire Testing ATTN: James F. O'Bryon Washington, DC 20301-3110
(Unclass., unlimited) 12 (Unclass., limited) 2 (Classified) 2	Administrator Defense Technical Info Center ATTN: DTIC-DDA Cameron Station Alexandria, VA 22304-6145
1	HQDA (SARD-TR) WASH DC 20310-0001
1	Commander US Army Materiel Command ATTN: AMCDRA-ST 5001 Eisenhower Avenue Alexandria, VA 22333-0001
1	Commander US Army Laboratory Command ATTN: AMSLC-DL Adelphi, MD 20783-1145
2	Commander Armament RD&E Center US Army AMCCOM ATTN: SMCAR-MSI Picatinny Arsenal, NJ 07806-5000
2	Commander Armament RD&E Center US Army AMCCOM ATTN: SMCAR-TDC Picatinny Arsenal, NJ 07806-5000
1	Director Benet Weapons Laboratory Armament RD&E Center US Army AMCCOM ATTN: SMCAR-CCB-TL Watervliet, NY 12189-4050
1	Commander US Army Armament, Munitions and Chemical Command ATTN: SMCAR-ESP-L Rock Island, IL 61299-5000
1	Commander US Army Aviation Systems Command ATTN: AMSAV-DACL 4300 Goodfellow Blvd. St. Louis, MO 63120-1798

No of Copies	Organization
1	Director US Army Aviation Research and Technology Activity Ames Research Center Moffett Field, CA 94035-1099
1	Commander US Army Missile Command ATTN: AMSMI-RD-CS-R (DOC) Redstone Arsenal, AL 35898-5010
1	Commander US Army Tank-Automotive Command ATTN: AMSTA-TSL (Technical Library) Warren, MI 48397-5000
1	Director US Army TRADOC Analysis Command ATTN: ATAA-SL White Sands Missile Range, NM 88002-5502
(Class. only) 1	Commandant US Army Infantry School ATTN: ATSH-CD (Security Mgr.) Fort Benning, GA 31905-5660
(Unclass. only) 1	Commandant US Army Infantry School ATTN: ATSH-CD-CSO-OR Fort Benning, GA 31905-5660
1	Air Force Armament Laboratory ATTN: AFATL/DLODL Eglin AFB, FL 32542-5000
	Aberdeen Proving Ground
2	Dir, USAMSAA ATTN: AMXSY-D AMXSY-MP, H. Cohen
1	Cdr, USATECOM ATTN: AMSTE-TO-F
3	Cdr, CRDEC, AMCCOM ATTN: SMCCR-RSP-A SMCCR-MU SMCCR-MSI
1	Dir, VLAMO ATTN: AMSLC-VL-D

No. of Copies	Organization
2	Commander US Army Laboratory Command ATTN: AMSLC-CG AMSLC-TR, R. Vitali 2800 Powder Mill Road Adelphi, MD 20783-1145
1	Commander Armament RD&E Center US Army AMCCOM ATTN: SMCAR-TSS Picatinny Arsenal, NJ 07806-5000
1	Commander US Army Missile Command ATTN: AMSTA-CG Redstone Arsenal, AL 35898-5000
1	Commander USA Concepts Analysis Agency ATTN: D. Hardison 8120 Woodmont Avenue Bethesda, MD 20014-2797
1	C.I.A. 101R/DB/Standard GE47 HQ Washington, DC 20505
1	Commander US Army War College ATTN: Library-FF229 Carlisle Barracks, PA 17013
1	US Army Ballistic Missile Defense Systems Command Advanced Technology Center P. O. Box 1500 Huntsville, AL 35807-3801
1	Commander US Army Materiel Command ATTN: AMCPM-GCM-WF 5001 Eisenhower Avenue Alexandria, VA 22333-5001
1	Commander US Army Materiel Command ATTN: AMCDE-DW 5001 Eisenhower Avenue Alexandria, VA 22333-5001
1	Commander US Army Watervliet Arsenal ATTN: SARWV-RD, R. Thierry Watervliet, NY 12189-5001

No. of Copies	Organization
3	Commander US Army Natick R&D Center ATTN: STRNC-OI Natick, MA 01760
1	Commander US Army Aviation Systems Command ATTN: AMSAV-ES 4300 Goodfellow Blvd. St. Louis, MO 63120-1798
1	Commander US Army Survivability Management Office ATTN: SLCSM-D 2800 Powder Mill Road Adelphi, MD 20783-1145
1	Commander CECOM R&D Technical Library ATTN: ASQNC-ELC-I-T, Myer Center Fort Monmouth, NJ 07703-5000
1	Commander US Army Harry Diamond Laboratories ATTN: SLCHD-TA-L 2800 Powder Mill Road Adelphi, MD 20783-1145
1	Commandant US Army Aviation School ATTN: Aviation Agency Fort Rucker, AL 36360
1	Project Manager US Army Tank-Automotive Command Improved TOW Vehicle ATTN: AMCPM-ITV Warren, MI 48397-5000
2	Project Manager M1 Abrams Tank System ATTN: AMCPM-ABMS-SA, T. Dean Warren, MI 48092-2498
1	Project Manager Fighting Vehicle Systems ATTN: AMCPM-BFVS Warren, MI 48092-2498
1	President US Army Armor & Engineer Board ATTN: ATZK-AD-S Fort Knox, KY 40121-5200

No. of Copies	Organization
1	Commander US Army Vulnerability Assessment Laboratory ATTN: SLCVA-CF White Sands Missile Range, NM 88002-5513
1	Project Manager M-60 Tank Development ATTN: AMCPM-ABMS Warren, MI 48092-2498
1	Commander US Army Training & Doctrine Command ATTN: ATCD-MA, MAJ Williams Fort Monroe, VA 23651
2	Commander US Army Materials Technology laboratory ATTN: SLCMT-ATL Watertown, MA 02172-0001
1	Commander US Army Research Office ATTN: Technical Library P. O. Box 12211 Research Triangle Park, NC 27709-2211
1	Commander US Army Belvoir R&D Center ATTN: STRBE-WC Fort Belvoir, VA 22060-5606
1	Commander US Army Logistics Management Center Defense Logistics Studies Fort Lee, VA 23801
1	Commandant US Army Command and General Staff College Fort Leavenworth, KS 66027
1	Commandant US Army Special Warfare School *ATTN: Rev & Tng Lit Div* Fort Bragg, NC 28307
1	Commander US Army Foreign Science & Technology Center ATTN: AMXST-MC-3 220 Seventh Street, NE Charlottesville, VA 22901-5396

No. of Copies	Organization
2	Commandant US Army Field Artillery Center & School ATTN: ATSF-CO-MW, B. Willis Fort Sill, OK 73503-5600
1	Office of Naval Research ATTN: Code 473, R. S. Miller 800 N. Quincy Street Arlington, VA 22217-9999
3	Commandant US Army Armor School ATTN: ATZK-CD-MS, M. Falkovitch Armor Agency Fort Knox, KY 40121-5215
2	Commander Naval Sea Systems Command ATTN: SEA 62R SEA 64 Washington, DC 20362-5101
1	Commander Naval Air Systems Command ATTN: AIR-954-Technical Library Washington, DC 20360
1	Naval Research Laboratory Technical Library Washington, DC 20375
1	Commander Naval Surface Warfare Center ATTN: Code DX-21 Technical Library Dahlgren, VA 22448-5000
1	Commander Naval Weapons Center ATTN: Information Science Division China Lake, CA 93555-6001
2	Superintendent Naval Postgraduate School Department of Mechanical Engineering Monterey, CA 93943-5100
1	Commander Naval Ordnance Station ATTN: Technical Library Indian Head, MD 20640-5000
1	AFSC/SDOA Andrews AFB, MD 20334

No. of Copies	Organization
1	AF Astronautics Laboratory AFAL/TSTL, Technical Library Edwards AFB, CA 93523-5000
1	AFATL/DLYV Eglin AFB, FL 32542-5000
1	AFATL/DLXP Eglin AFB, FL 32542-5000
1	AFATL/DLJE Eglin AFB, FL 32542-5000
1	NASA/Lyndon B. Johnson Space Center ATTN: NHS22 Library Section Houston, TX 77054
1	FTD/NIIS Wright-Patterson AFB, OH 45433
1	Director Lawrence Livermore Laboratory ATTN: Technical Information Department L-3 P. O. Box 808 Livermore, CA 94550
2	Director Los Alamos Scientific Laboratory ATTN: Document Control for Reports Library P. O. Box 1663 Los Alamos, NM 87544
1	Director Sandia Laboratories ATTN: Document Control for 3141 Sandia Report Collection Albuquerque, NM 87115
1	Director Sandia Laboratories Livermore Laboratory ATTN: Document Control for Technical Library P. O. Box 969 Livermore, CA a94550
1	Director National Aeronautics and Space Administration Scientific & Technical Information Facility P. O. Box 8757 Baltimore/Washington International Airport MD 21240

No. of Copies	Organization
1	Aerospace Corporation ATTN: Technical Information Services P. O. Box 92957 Los Angeles, CA 90009
1	The Boeing Company ATTN: Aerospace Library P. O. Box 3707 Seattle, WA 98124
1	Director Institute for Defense Analyses ATTN: Library 1801 Beauregard Street Alexandria, VA 22311
1	Battelle Memorial Institute ATTN: Technical Library 505 King Avenue Columbus, OH 43201-2693
1	Johns Hopkins University Applied Physics Laboratory ATTN: Jonathan Fluss John Hopkins Road Laurel, MD 20707-0690
1	Pennsylvania State University Department of Mechanical Engineering ATTN: K. Kuo University Park, PA 16802-7501
1	SRI International Propulsion Sciences Division ATTN: Technical Library 333 Ravenswood Avenue Menlo Park, CA 94025-3493
1	Rensselaer Polytechnic Institute Department of Mathematics Troy, NJ 12181
1	Eichelberger Consulting Company ATTN: Dr. R. Eichelberger, President 409 West Catherine Street Bel Air, MD 21014
1	FMC Corporation Aberdeen Regional Office ATTN: Leland Watermeier Bel Air, MD 21014

Aberdeen Proving Ground

12 Dir, USAMSAA
ATTN: AMXSY-A, W. Clifford
J. Meredith
AMXSY-C, A. Reid
AMXSY-CS, P. Beavers
C. Cairns
D. Frederick
AMXSY-G, J. Kramer
AMXSY-GA, W. Brooks
AMXSY-J, A. LaGrange
AMXSY-L, J. McCarthy
AMXSY-RA, R. Scungio
M. Smith

3 Cdr, USATECOM
ATTN: AMSTE-SI-F
AMSTE-LFT, D. Gross
R. Harrington

1 Cdr, CSTA
ATTN: STECS

INTENTIONALLY LEFT BLANK.

USER EVALUATION SHEET/CHANGE OF ADDRESS

This Laboratory undertakes a continuing effort to improve the quality of the reports it publishes. Your comments/answers to the items/questions below will aid us in our efforts.

1. BRL Report Number BRL-TR-3084 Date of Report APR 90

2. Date Report Received _____

3. Does this report satisfy a need? (Comment on purpose, related project, or other area of interest for which the report will be used.) _____

4. Specifically, how is the report being used? (Information source, design data, procedure, source of ideas, etc.) _____

5. Has the information in this report led to any quantitative savings as far as man-hours or dollars saved, operating costs avoided, or efficiencies achieved, etc? If so, please elaborate. _____

6. General Comments. What do you think should be changed to improve future reports? (Indicate changes to organization, technical content, format, etc.) _____

CURRENT ADDRESS

Name

Organization

Address

City, State, Zip Code

7. If indicating a Change of Address or Address Correction, please provide the New or Correct Address in Block 6 above and the Old or Incorrect address below.

OLD ADDRESS

Name

Organization

Address

City, State, Zip Code

(Remove this sheet, fold as indicated, staple or tape closed, and mail.)

FOLD HERE

DEPARTMENT OF THE ARMY

Director
U.S. Army Ballistic Research Laboratory
ATTN: SLCBR-DD-T
Aberdeen Proving Ground, MD 210[illegible]-5066
OFFICIAL BUSINESS

NO POSTAGE
NECESSARY
IF MAILED
IN THE
UNITED STATES

BUSINESS REPLY MAIL
FIRST CLASS PERMIT No 0001, APG, MD

POSTAGE WILL BE PAID BY ADDRESSEE

Director
U.S. Army Ballistic Research Laboratory
ATTN: SLCBR-DD-T
Aberdeen Proving Ground, MD 21005-9989

FOLD HERE